HHS Public Access

Author manuscript

Bone. Author manuscript; available in PMC 2015 March 13.

Published in final edited form as:

Bone. 2014 February ; 59: 229–234. doi:10.1016/j.bone.2013.11.026.

Ovariectomy Enhances Mechanical Load-Induced Solute Transport around Osteocytes in Rat Cancellous Bone

Cesare Ciani[a], **Divya Sharma**[a], **Stephen B. Doty**[b], and **Susannah P. Fritton**[a,*]

[a]Department of Biomedical Engineering, City College of New York, New York, NY 10031 USA

[b]Research Division, Hospital for Special Surgery, New York, NY 10021 USA

Abstract

To test if osteoporosis alters mechanical load-induced interstitial fluid flow in bone, this study examined the combined effect of estrogen deficiency and external loading on solute transport around osteocytes. An in vivo tracer, FITC-labeled bovine serum albumin, was injected into anaesthetized ovariectomized and control female Sprague Dawley rats before the right tibia was subjected to a controlled, physiological, non-invasive sinusoidal load to mimic walking. Tracer movement through the lacunar-canalicular system surrounding osteocytes was quantified in cortical and cancellous bone from the proximal tibia using confocal microscopy, with the non-loaded tibia serving as internal control. Overall, the application of mechanical loading increased the percentage of osteocyte lacunae labeled with injected tracer, and ovariectomy further enhanced movement of tracer. An analysis of separate regions demonstrated that ovariectomy enhanced in vivo transport of the injected tracer in the cancellous bone of the tibial epiphysis and metaphysis but not in the cortical bone of the metaphysis. These findings show that bone changes due to reduced estrogen levels alter convectional transport around osteocytes in cancellous bone and demonstrate a functional difference of interstitial fluid flow around osteocytes in estrogen-deficient rats undergoing the same physical activity as controls. The altered interstitial fluid flow around osteocytes is likely related to nanostructural matrix-mineral level differences recently demonstrated at the lacunar-canalicular surface of estrogen-deficient rats, which could affect the transmission of mechanical loads to the osteocyte.

Keywords

osteoporosis; osteocyte; canaliculi; interstitial fluid; perilacunar remodeling; mechanotransduction

*Corresponding author: Department of Biomedical Engineering, City College of New York, 160 Convent Avenue, New York, NY 10031, Phone: 212-650-5213, Fax: 212-650-6727, fritton@ccny.cuny.edu.

Conflict of interest statement

The authors have no conflicts of interest.

1. Introduction

Bone is a porous, dynamic cellular structure that can adapt to accommodate changes in its functional environment. The lacunar-canalicular porosity is a complex web of lacunae and canaliculi in the mineralized matrix that houses the osteocytes and their processes, forming a syncytium that connects osteocytes and cells located on bone surfaces [1]. The anatomical location of osteocytes and the extended connections throughout bone tissue make the osteocyte the ideal candidate to perceive and respond to mechanical stimuli [2, 3].

When bone is mechanically loaded, fluid pressure gradients are induced in the bone pores, creating a load-induced interstitial fluid displacement in the lacunar-canalicular porosity [4, 5]. Load-induced interstitial fluid movement affects osteocytes by enhancing solute transport via a convection mechanism that ensures the adequate metabolic function of bone cells, which is crucial for bone maintenance and adaptation [6–9]. Load-induced interstitial fluid movement is also believed to play a role in bone's mechanosensory system via its role in the transduction of whole-bone forces to the osteocyte process cytoskeleton via transmembrane links from the osteocyte to the canalicular wall [10–13]. To demonstrate bone's interstitial fluid pathway, we and several other groups have performed in vivo vascular injection of different tracers, such as microperoxidase, ferritin, reactive red, and procion red [14–20]. The same experimental approach has been used to demonstrate enhanced mass transport through the lacunar-canalicular system due to applied mechanical loading [21–24].

While weight-bearing exercise has been shown to be important in bone maintenance [2], estrogen also protects the skeleton from bone loss by suppressing bone turnover and maintaining a balance between formation and resorption [25]. A reduction of estrogen levels has been shown to induce osteocyte death via apoptosis in mice, rats, sheep, and humans [26–29]. This decrease in osteocyte viability could alter the interconnectedness of the osteocyte network, affecting interstitial fluid flow and altering the mechanical stimulus experienced by the bone cells [30–34]. Recent results from our lab analyzing changes in the osteocyte microenvironment due to ovariectomy (OVX) in the rat demonstrate nanostructural matrix-mineral level differences like loose collagen surrounding osteocyte lacunae and canaliculi [35]. These changes appear to make OVX bone tissue more permeable to small molecules at the lacunar-canalicular surface, which could potentially alter interstitial fluid flow around osteocytes during mechanical loading. The goal of the present study was to investigate the functional significance of a more permeable osteocyte microenvironment induced in the estrogen-deficient state.

This study tested the hypothesis that estrogen deficiency alters bone interstitial fluid movement through the osteocyte lacunar-canalicular network. Solute transport around osteocytes was measured in ovariectomized rats and compared to control rats undergoing a similar level of mechanical loading. A controlled, non-invasive, dynamic load that mimicked walking was applied to the right tibia immediately after the injection of a fluorescent tracer. Tracer distribution in the interstitial fluid space surrounding osteocytes was analyzed in cortical and cancellous bone from the proximal tibia, a region that undergoes bone loss when ovarian function is impaired in both humans and animal models [36, 37].

2. Materials and methods

Permission for the study was granted by the Institutional Animal Care and Use Committees at the Hospital for Special Surgery and the City College of New York. A non-invasive device was used to apply mechanical loads to the rat hindlimb (ElectroForce TestBench, Bose Corp., Minnetonka, MN) similar to a tibial loading device previously developed in the mouse [38].

2.1 Loading device calibration

To calibrate the loading device, strain gages were applied to the tibia of female Sprague Dawley rats (n=3; 26 weeks old; 305 ± 18g; Harlan Laboratories, Indianapolis, IN). The animals were anaesthetized with isoflurane, and the right medial proximal diaphysis of the tibia was surgically exposed. This anatomical location was chosen for its lack of muscle attachments and flat surface, which could accommodate application of a strain gage. The tibial surface was scraped with a scalpel to remove the periosteal layer, and then it was cleaned and dehydrated with 100% ethanol and acetone. A single-element foil gage (CEA-032UW-120, Vishay Micro-Measurements, Raleigh, NC) was aligned with the tibial long axis and attached using cyanoacrylate. The rat's right lower limb was then placed between the knee and foot holder of the loading device and a compressive pre-load of 1 N was applied to maintain the limb's position (Fig. 1a). To produce physiological strains in the tibia [39, 40], axial sinusoidal loads were applied at 1 Hz using four peak magnitudes ranging from 9 to 18 N to determine the load-microstrain relationship. The applied load of 14 N at 1 Hz used in the subsequent loading protocol to simulate slow walking generated approximately 500 microstrain at the medial proximal diaphysis of the tibia (Fig. 1b).

2.2 Animal model and experimental design

To assess the effects of loss of ovarian function on mass transport due to mechanical loading, the rat ovariectomy model was utilized to induce osteopenia. Twenty-week-old rats were used to avoid the rapid growth stage associated with significant bone turnover in the proximal tibia [41]. Female Sprague Dawley rats (Harlan Laboratories, Indianapolis, IN) were divided into two groups at 20 weeks of age, with one group undergoing ovariectomy (OVX, n=6), and the other group subjected to sham surgery (SHAM, n=6), consisting of the surgical exposure of the ovaries without removal. After a one-week recovery period, the OVX group was pair-fed to the average food intake of the SHAM group for five weeks prior to load application to reduce weight gain caused by OVX [42]. Solute transport around osteocytes was assessed six weeks post-OVX to allow bone loss to develop in the proximal tibia [37].

2.3 Application of mechanical loading

One short-duration loading bout was applied to both SHAM and OVX groups six weeks post-surgery. After recording body weight, the rats were anaesthetized via an intraperitoneal injection of a mixture of ketamine (75 mg/kg body weight), and xylazine (10 mg/kg body weight). The left jugular vein was exposed surgically and a 25G 5/8″ needle attached to a 3-ml syringe was inserted into the vein to inject a bolus (~2 ml) of tracer solution of FITC-labeled bovine serum albumin (67 kDa, diameter ~7 nm, dosage of 0.25 mg/g body weight;

#A9771, Sigma-Aldrich, St. Louis, MO). Immediately after the tracer injection (injection time 2 minutes) a sinusoidal load was applied to the right tibia using the non-invasive mechanical loading device. The applied loading magnitude of 14 N, and the loading duration and frequency (100 cycles at 1 Hz), were chosen to mimic a short period of slow walking activity (total loading time: 100 s) [39, 40]. Immediately after load application the rats were sacrificed with carbon dioxide inhalation and the loaded and unloaded contralateral tibiae were harvested and put into fixative (0.5% gluteraldehyde, 2% paraformaldehyde in 0.05M cacodylate-sodium buffer, pH 7.4) for 48 hours. To confirm the effectiveness of the OVX procedure, ovary removal was visually verified, and the uterine horns were weighed.

2.4 Histological processing, imaging techniques, and data collection

Cortical and cancellous bone samples were analyzed from the metaphysis and epiphysis of the proximal tibia. Tibial blocks were cut 3 mm distal to the growth plate and embedded in PMMA after 48 hours of fixation. Either sagittal or frontal tibial sections (400–600 μm) were cut with a diamond-blade saw. Sections were then ground down to a final thickness of 40–70 μm using Carbimet paper discs (800 and 1200 grit; Buehler, Lake Bluff, IL), dried in ascending graded ethanol (75%, 95%, and 100%, 5 minutes each), and coverslipped with mounting media (Richard-Allan Scientific, Kalamazoo, MI).

To visualize tracer labeling, 20 regions were analyzed for each tibia (both loaded and unloaded): 5 regions from the cancellous metaphysis, 5 from the cancellous epiphysis, and 10 from the cortical metaphysis (Fig. 2). The cortical regions were visualized using a confocal microscope with a 40× oil immersion lens (Leica TCS SP2, Germany, 1.25 numerical aperture, 630 gain, 2.4 offset, and pinhole set at 1 Airy unit, wavelength excitation of 488 nm, and laser intensity set to 15%); images were taken at a resolution of 2048 × 2048 pixels with a field view of 375 μm × 375 μm. The cancellous regions were visualized using the same parameters used for the cortical regions with the only difference being a 2× factor in the objective; thus the field of view was 187.5 μm × 187.5 μm.

To determine the percentage of osteocyte lacunae labeled with the injected tracer, the total number of osteocyte lacunae was first counted for each confocal image using ImageJ (NIH). The confocal images were then transformed to grayscale intensity and thresholded. For both the cortical and cancellous bone, the threshold value was determined from images of the unloaded limb and then used in the corresponding images of the mechanically loaded limb. The osteocyte lacunae were counted as labeled if at least 80% of the lacunar space or 80% of the periphery of the lacuna was stained (Fig. 3). Then the number of labeled lacunae in each image was divided by the total number of lacunae in the image to determine the percentage of osteocyte lacunae labeled. During processing the analyzer was blinded to treatment group.

2.5 Statistical analyses

For each tibia (both loaded and unloaded), the percentage of osteocyte lacunae labeled was averaged for the regions analyzed in each anatomical location (5 cancellous metaphysis regions, 5 cancellous epiphysis regions, and 10 cortical metaphysis regions). A total average for each tibia, with all regions pooled, was also calculated. Group averages were then

calculated for the SHAM and OVX groups. All results are reported as mean ± standard deviation.

To examine the effects of mechanical loading and loss of ovarian function on tracer movement for the three anatomical locations (cortical metaphysis, cancellous metaphysis, and cancellous epiphysis), data were analyzed using a two-way repeated-measures analysis of variance (ANOVA), with the within-subject factor the loading condition (unloaded and loaded tibiae) and the between-subject factor the treatment (SHAM and OVX). Differences in percentage of osteocyte lacunae labeled with the injected tracer with all the regions pooled was also assessed using two-way repeated-measures ANOVA. All data sets were confirmed to have a normal distribution before using parametric tests, and Holm-Sidak post-hoc t-tests were used to determine differences between groups. For comparison of uterine horn and body weights in SHAM and OVX, unpaired, two-tailed t-tests were used. All statistical analyses were performed using Prism 6 (GraphPad Software Inc., San Diego, CA) with a significance level of $p < 0.05$.

3. Results

The effectiveness of ovariectomy was verified by the absence of ovaries and by the reduced dimension and weight of the uterine horns in the ovariectomized rats (SHAM: 0.61 ± 0.13 g, OVX: 0.14 ± 0.033 g; $p < 0.05$). Despite pair-feeding starting one week post-surgery, at the time of the load application (six weeks post-surgery) the OVX rats weighed more than the age-matched, sham-operated rats (SHAM: 265 ± 12 g, OVX: 302 ± 17 g; $p < 0.05$).

Overall, the externally applied loading increased the percentage of osteocyte lacunae labeled with injected tracer in both SHAM and OVX. Pooling together the three proximal tibia regions, loading caused an increase in percentage of osteocyte lacunae labeled compared to the unloaded, contralateral tibia (SHAM: +129%, OVX: +175%, Fig. 4). Separate analysis of each region (cortical metaphysis, cancellous metaphysis, and cancellous epiphysis) demonstrated that the applied loading significantly enhanced tracer transport for all three locations in both groups except for the cancellous epiphysis of the SHAM group (Fig. 5). The cortical metaphysis showed the least solute transport enhancement due to applied loading (SHAM: +63%, OVX: +120%) compared to the cancellous bone in the metaphysis (SHAM: +178%, OVX: +145%) and cancellous bone in the epiphysis (OVX: +327%).

Ovariectomy further enhanced overall movement of tracer into the lacunar-canalicular porosity in the proximal tibia due to applied loading, with the percentage of osteocyte lacunae labeled with tracer for loaded OVX greater than loaded SHAM (+59%, Fig. 4). Separate analysis of each region demonstrated that this overall increase in labeled osteocyte lacunae in loaded tibiae of the OVX group compared to the loaded SHAM was due to an increase in labeled lacunae in the cancellous bone of the epiphysis and metaphysis (+66% and +142%, respectively, Fig. 5). There was no solute transport enhancement due to ovariectomy in cortical bone of the metaphysis (Fig. 5).

4. Discussion

Although it has been proposed that a loss in osteocyte viability due to estrogen deficiency might reduce the interconnectedness of the lacunar-canalicular network, we found no negative impact of ovariectomy on interstitial fluid flow around osteocytes. Instead, this study demonstrates that estrogen deficiency enhances interstitial fluid flow through the lacunar-canalicular porosity surrounding osteocytes in the proximal rat tibia. Solute transport was increased in cancellous bone of the proximal metaphysis and epiphysis in response to physiological mechanical loading, whereas in cortical bone of the proximal tibia solute transport was the same in normal and estrogen-deficient rats.

While the effect of applied mechanical loading on periosteocytic solute transport has not been reported for animals in an estrogen-deficient state, our results for the sham-operated control group show increased transport similar to that of previous studies in non-treated bone. A study that applied external loading to the rat tibia using four-point bending demonstrated an increase in the number of periosteocytic spaces labeled with injected tracer compared to the unloaded, contralateral tibia [21]. The enhancement of transport varied across the tibia mid-diaphysis, with more labeled periosteocytic spaces found in the portion of the mid-diaphysis subjected to tension, a region that experienced higher strains under the bending load compared to the portion of the mid-diaphysis that underwent compression. Recent work using fluorescence recovery after photobleaching (FRAP) in freshly harvested murine tibiae demonstrated a 31% increase in the transport of a small molecular-weight tracer due to applied mechanical loading using a physiological loading magnitude similar to that used in the present study [24]. In the present study a higher overall increase in solute transport (+129%) was found for the control rats (SHAM group), which may be related to the difference in assessment methods compared to previous studies, as well as the inclusion of cancellous bone, which was not examined in previous studies.

In the present study the same controlled external force was applied to both SHAM and OVX groups to mimic the same physical activity (walking); we did not attempt to apply the same bone strains to the two groups. Nor did we investigate the effect of loading frequency on tracer transport. Rather, we investigated whether a physiological activity performed after OVX-induced bone loss altered solute and fluid transport in the osteocyte lacunar-canalicular system. As with many studies using the OVX rat model, the OVX group weighed more six weeks after ovariectomy than the age-matched SHAM group (+14%), despite pair feeding starting one week post-OVX. It has been shown that pair feeding reduces ovariectomy-induced weight gain in the rat, but it does not prevent increased weight gain compared to age-matched controls [42]. The weight gain in OVX rats has been suggested to provide partial protection from bone loss due to estrogen deficiency [42].

While not assessed in the present study, the Sprague Dawley rat OVX model produces a decreased bone volume fraction in the cancellous bone of the proximal tibial metaphysis of approximately 50% over the time course used in this study [43]. Bone loss in the metaphysis region could produce higher strains in the remaining cancellous bone when the external load is applied, which could increase solute transport. However, increased solute transport was also found in cancellous bone of the tibial epiphysis of the OVX group. Because the

epiphysis region does not exhibit bone loss due to ovariectomy, bone strains should not be significantly elevated in the OVX group in this region [44]. Thus an increased strain level might contribute to enhanced solute transport in cancellous bone of the metaphysis, but it does not explain the enhanced solute transport in the epiphysis. The delivery of tracer to the bone tissue is also dependent on the bone vasculature, which may be altered after OVX [45]. However, the effect of mechanical loading was always assessed relative to the contralateral, unloaded tibiae such that changes in baseline delivery of tracer in the OVX group would be taken into account. In addition, no significant differences in tracer transport were found in unloaded OVX and SHAM bones (Fig. 5), leading to the conclusion that baseline delivery of tracer through the bone vasculature was similar in both conditions.

The enhanced load-induced solute transport in the OVX group is likely related to microarchitectural changes recently found in the osteocyte lacunar-canalicular system of estrogen-deficient rats. Results from our lab analyzing changes in the osteocyte microenvironment due to ovariectomy have demonstrated a larger effective lacunar-canalicular porosity surrounding osteocytes in both cortical and cancellous bone from the proximal tibial metaphysis [35]. This increase in effective lacunar-canalicular porosity was due to nanostructural alterations at the lacunar-canalicular wall that make the bone matrix around osteocytes more permeable to small tracers. While alterations in the lacunar-canalicular surface were found throughout cancellous bone from the proximal tibial metaphysis in the rat OVX model, lacunar-canalicular changes were only found in certain regions of the cortical metaphysis, particularly in lamellar regions, and not in the older trabecular remnants [35]. In the present study these areas of cortical bone were not delineated; thus, it is possible that the lack of enhanced solute transport in OVX cortical bone in the present study is due to the sampling locations. In addition, in our previous study the lacunar-canalicular porosity in the cancellous bone from the proximal tibial epiphysis was not significantly increased after OVX, so we did not examine lacunar-canalicular surfaces in that region [35]. Thus it is not clear how the enhanced solute transport in the cancellous bone from the epiphysis demonstrated in the present study relates to microarchitectural changes due to OVX.

Although the mechanisms by which the changes in the osteocyte microenvironment demonstrated in the OVX rat model occur have not been established, the changes may be due to perilacunar/canalicular remodeling or osteocytic osteolysis, a process whereby osteocytes modify their immediate environment by removing mineralized matrix [46, 47]. It has been shown that under certain conditions, including parathyroid hormone administration, glucocorticoid administration, and lactation, osteocytes can respond to the new environmental status by altering their perilacunar space [46–49]. During lactation it has recently been shown that osteocytes can remove perilacunar mineral in a similar way that osteoclasts do, via secretion of tartrate-resistant acid phosphatase (TRAP) and cathepsin K [47]. Another recent study has demonstrated that matrix metalloproteinase (MMP)-13 is required for osteocyte perilacunar remodeling [50]. Even a slight resorption of the lacunar and canalicular surfaces surrounding osteocytes would result in a broadening of the lacunar and canalicular spaces, and the larger pores would allow a larger volume of fluid to move during cyclic or pulsatile loading. A larger amount of tracer would be transported to the lacunae when bone is more permeable because the fluid displacement and the volume of

fluid exchange during cyclic loading increases with increasing lacunar-canalicular permeability [9]. Thus, perilacunar/canalicular remodeling could enhance molecular transport through the lacunar-canalicular network, with consequent increase in the number of osteocyte lacunae labeled with injected tracer. Further work is required to assess whether osteocyte-related changes such as increased TRAP or cathepsin K expression or changes in fluorochrome labeling around osteocytes occur after ovariectomy.

While not assessed in the present study, the alteration in tracer movement through the lacunar-canalicular system may also be related to the decrease of defense against oxidative stress caused by estrogen loss [25]. Mechanical stimulation has been shown to preserve osteocyte viability via activation of extracellular signal-related kinases (ERKS), requiring integrin engagement [51]. Estrogen deficiency has also been linked to reduced estrogen receptor (ERα) expression and activity, and the integrin signaling pathway has been shown to be downregulated in OVX mice [52]. Recent analysis of estrogen-deficient mice has also shown that osteocyte apoptosis occurs in discrete regions of the femur, in older regions that may have accumulated more oxidative stress [29]. It has also been suggested, and has been shown in a damage model [53], that surviving osteocytes surrounding apoptotic osteocytes signal via RANKL to initiate osteoclast recruitment [29]. Thus there is increasing evidence that there may be a link between estrogen loss and the response of the osteocyte to the ensuing increase of metabolic stress via apoptosis and perilacunar/canalicular remodeling, but delineating how these processes are related requires further investigation.

The results of this study as well as our recent assessment of changes to the osteocyte microenvironment [35] suggest that estrogen deficiency may affect the bone mechanotransduction process in two ways. First, the results of this study provide a mechanism by which the transduction of mechanical loading to osteocytes could be altered. It has been hypothesized that the diminished ability to maintain bone strength in postmenopausal osteoporosis is a failure of bone's normal adaptive properties to remodel in response to functional loading [54]. Alteration of the interstitial fluid space around osteocytes in the estrogen-deficient state may affect the mechanosensitivity of osteocytes. Osteocyte cell processes have been demonstrated to be connected to the canalicular wall through tethering elements and integrin connections [12, 13]. The proposed function of these structures is to work as a cellular strain amplifier that is activated during fluid flow [11, 12]. If the tethering elements and integrin attachments were disrupted, the capability of the osteocyte to perceive mechanical stimuli could be impaired. Second, the increased solute transport demonstrated in this study is likely due to a change in permeability of the osteocyte lacunar-canalicular walls [35]. While not measured here, it is also possible that the alterations of the lacunar-canalicular mineralized matrix surface demonstrated in [35], e.g., collagen intruding into the interstitial space, may alter the fluid velocity profiles around osteocytes during mechanical loading [9]. Combined with potential alteration in connections between the osteocyte and the canalicular wall, the mechanical forces transmitted to the osteocytes via interstitial fluid flow could be diminished, thus reducing the ability of the osteocyte to respond to mechanical loading.

In conclusion, this study demonstrates enhanced in vivo convectional transport of an injected tracer due to applied mechanical loading, demonstrating a functional difference of

interstitial fluid flow around osteocytes in cancellous bone of estrogen-deficient rats undergoing the same physical activity as controls. The altered interstitial fluid flow around osteocytes is likely related to nanostructural matrix-mineral level differences recently demonstrated at the lacunar-canalicular surface of estrogen-deficient rats, which could affect the transmission of mechanical loads to the osteocyte. Further investigation of the microstructural changes of the lacunar-canalicular porosity as well as characterization of osteocyte viability and changes in tissue permeability are needed to determine whether loss of ovarian function may impair the capability of osteocytes to perform efficiently as mechanotransducers due to changes in the osteocyte microenvironment and interstitial fluid flow.

Acknowledgments

This study was supported by a grant from the NIH (NIAMS, AR052866). The authors thank Adriana Larriera, M.S. for assistance with image processing and J. Christopher Fritton, Ph.D. for assistance with fixture design and calibration of the loading device.

References

1. Hancox, NM. Biology of Bone. Cambridge, England: Cambridge University Press; 1972.
2. Cowin SC, Moss-Salentijn L, Moss ML. Candidates for the mechanosensory system in bone. J Biomech Eng. 1991; 113:191–7. [PubMed: 1875693]
3. Lanyon LE. Osteocytes, strain detection, bone modeling and remodeling. Calcif Tissue Int. 1993; 53 (Suppl 1):S102–6. [PubMed: 8275362]
4. Qin YX, Lin W, Rubin C. The pathway of bone fluid flow as defined by in vivo intramedullary pressure and streaming potential measurements. Ann Biomed Eng. 2002; 30:693–702. [PubMed: 12108843]
5. Fritton SP, Weinbaum S. Fluid and solute transport in bone: flow-induced mechanotransduction. Annu Rev Fluid Mech. 2009; 41:347–74. [PubMed: 20072666]
6. Piekarski K, Munro M. Transport mechanism operating between blood supply and osteocytes in long bones. Nature. 1977; 269:80–2. [PubMed: 895891]
7. Knothe Tate ML, Knothe U, Niederer P. Experimental elucidation of mechanical load-induced fluid flow and its potential role in bone metabolism and functional adaptation. Am J Med Sci. 1998; 316:189–95. [PubMed: 9749561]
8. Dodd JS, Raleigh JA, Gross TS. Osteocyte hypoxia: a novel mechanotransduction pathway. Am J Physiol. 1999; 277:C598–602. [PubMed: 10484347]
9. Wang L, Cowin SC, Weinbaum S, Fritton SP. Modeling tracer transport in an osteon under cyclic loading. Ann Biomed Eng. 2000; 28:1200–9. [PubMed: 11144981]
10. Burger EH, Klein-Nulend J. Mechanotransduction in bone--role of the lacuno-canalicular network. Faseb J. 1999; 13 (Suppl):S101–12. [PubMed: 10352151]
11. Han Y, Cowin SC, Schaffler MB, Weinbaum S. Mechanotransduction and strain amplification in osteocyte cell processes. Proc Natl Acad Sci U S A. 2004; 101:16689–94. [PubMed: 15539460]
12. Wang Y, McNamara LM, Schaffler MB, Weinbaum S. A model for the role of integrins in flow induced mechanotransduction in osteocytes. Proc Natl Acad Sci U S A. 2007; 104:15941–6. [PubMed: 17895377]
13. McNamara LM, Majeska RJ, Weinbaum S, Friedrich V, Schaffler MB. Attachment of osteocyte cell processes to the bone matrix. Anat Rec (Hoboken). 2009; 292:355–363. [PubMed: 19248169]
14. Doty, SB.; Schofield, BH. Metabolic and structural changes within osteocytes of rat bone. In: Talmage, RV.; Munson, PL., editors. Calcium, Parathyroid Hormone and the Calcitonins. Amsterdam: Excerpta Medica; 1972. p. 353-64.
15. Tanaka T, Sakano A. Differences in permeability of microperoxidase and horseradish peroxidase into the alveolar bone of developing rats. J Dent Res. 1985; 64:870–6. [PubMed: 3858312]

16. Montgomery RJ, Sutker BD, Bronk JT, Smith SR, Kelly PJ. Interstitial fluid flow in cortical bone. Microvasc Res. 1988; 35:295–307. [PubMed: 3393091]
17. Knothe Tate ML, Niederer P, Knothe U. In vivo tracer transport through the lacunocanalicular system of rat bone in an environment devoid of mechanical loading. Bone. 1998; 22:107–17. [PubMed: 9477233]
18. Qin L, Mak AT, Cheng CW, Hung LK, Chan KM. Histomorphological study on pattern of fluid movement in cortical bone in goats. Anat Rec. 1999; 255:380–7. [PubMed: 10409810]
19. Wang L, Ciani C, Doty SB, Fritton SP. Delineating bone's interstitial fluid pathway in vivo. Bone. 2004; 34:499–509. [PubMed: 15003797]
20. Ciani C, Doty SB, Fritton SP. Mapping bone interstitial fluid movement: displacement of ferritin tracer during histological processing. Bone. 2005; 37:379–87. [PubMed: 15964255]
21. Knothe Tate ML, Steck R, Forwood MR, Niederer P. In vivo demonstration of load-induced fluid flow in the rat tibia and its potential implications for processes associated with functional adaptation. J Exp Biol. 2000; 203:2737–45. [PubMed: 10952874]
22. Mak AF, Qin L, Hung LK, Cheng CW, Tin CF. A histomorphometric observation of flows in cortical bone under dynamic loading. Microvasc Res. 2000; 59:290–300. [PubMed: 10684735]
23. Tami AE, Schaffler MB, Knothe Tate ML. Probing the tissue to subcellular level structure underlying bone's molecular sieving function. Biorheology. 2003; 40:577–90. [PubMed: 14610309]
24. Price C, Zhou X, Li W, Wang L. Real-time measurement of solute transport within the lacunar-canalicular system of mechanically loaded bone: direct evidence for load-induced fluid flow. J Bone Miner Res. 2011; 26:277–85. [PubMed: 20715178]
25. Almeida M, Han L, Martin-Millan M, Plotkin LI, Stewart SA, Roberson PK, Kousteni S, O'Brien CA, Bellido T, Parfitt AM, Weinstein RS, Jilka RL, Manolagas SC. Skeletal involution by age-associated oxidative stress and its acceleration by loss of sex steroids. J Biol Chem. 2007; 282:27285–97. [PubMed: 17623659]
26. Tomkinson A, Reeve J, Shaw RW, Noble BS. The death of osteocytes via apoptosis accompanies estrogen withdrawal in human bone. J Clin Endocrinol Metab. 1997; 82:3128–35. [PubMed: 9284757]
27. Tomkinson A, Gevers EF, Wit JM, Reeve J, Noble BS. The role of estrogen in the control of rat osteocyte apoptosis. J Bone Miner Res. 1998; 13:1243–50. [PubMed: 9718192]
28. Brennan O, Kennedy OD, Lee TC, Rackard SM, O'Brien FJ. Effects of estrogen deficiency and bisphosphonate therapy on osteocyte viability and microdamage accumulation in an ovine model of osteoporosis. J Orthop Res. 2011; 29:419–24. [PubMed: 20886644]
29. Emerton KB, Hu B, Woo AA, Sinofsky A, Hernandez C, Majeska RJ, Jepsen KJ, Schaffler MB. Osteocyte apoptosis and control of bone resorption following ovariectomy in mice. Bone. 2010; 46:577–83. [PubMed: 19925896]
30. Weinstein RS, Manolagas SC. Apoptosis and osteoporosis. Am J Med. 2000; 108:153–64. [PubMed: 11126309]
31. Klein-Nulend J, Nijweide PJ, Burger EH. Osteocyte and bone structure. Curr Osteoporos Rep. 2003; 1:5–10. [PubMed: 16036059]
32. Knothe Tate ML, Adamson JR, Tami AE, Bauer TW. The osteocyte. Int J Biochem Cell Biol. 2004; 36:1–8. [PubMed: 14592527]
33. O'Brien CA, Jia D, Plotkin LI, Bellido T, Powers CC, Stewart SA, Manolagas SC, Weinstein RS. Glucocorticoids act directly on osteoblasts and osteocytes to induce their apoptosis and reduce bone formation and strength. Endocrinology. 2004; 145:1835–41. [PubMed: 14691012]
34. Bonewald LF. Osteocyte biology: its implications for osteoporosis. J Musculoskelet Neuronal Interact. 2004; 4:101–4. [PubMed: 15615083]
35. Sharma D, Ciani C, Marin PA, Levy JD, Doty SB, Fritton SP. Alterations in the osteocyte lacunar-canalicular microenvironment due to estrogen deficiency. Bone. 2012; 51:488–97. [PubMed: 22634177]
36. Frost HM, Jee WS. On the rat model of human osteopenias and osteoporoses. Bone Miner. 1992; 18:227–36. [PubMed: 1392696]

37. Wronski TJ, Dann LM, Scott KS, Cintron M. Long-term effects of ovariectomy and aging on the rat skeleton. Calcif Tissue Int. 1989; 45:360–6. [PubMed: 2509027]
38. Fritton JC, Myers ER, Wright TM, van der Meulen MC. Loading induces site-specific increases in mineral content assessed by microcomputed tomography of the mouse tibia. Bone. 2005; 36:1030–8. [PubMed: 15878316]
39. Fritton, SP.; Rubin, CT. In vivo measurement of bone deformations using strain gages. In: Cowin, SC., editor. Bone Mechanics Handbook. CRC Press; 2001. p. 8.1-8.41.
40. Rabkin BA, Szivek JA, Schonfeld JE, Halloran BP. Long-term measurement of bone strain in vivo: the rat tibia. J Biomed Mater Res. 2001; 58:277–81. [PubMed: 11319741]
41. Horton JA, Bariteau JT, Loomis RM, Strauss JA, Damron TA. Ontogeny of skeletal maturation in the juvenile rat. Anat Rec (Hoboken). 2008; 291:283–92. [PubMed: 18228587]
42. Wronski TJ, Schenck PA, Cintron M, Walsh CC. Effect of body weight on osteopenia in ovariectomized rats. Calcif Tissue Int. 1987; 40:155–9. [PubMed: 3105846]
43. Laib A, Kumer JL, Majumdar S, Lane NE. The temporal changes of trabecular architecture in ovariectomized rats assessed by MicroCT. Osteoporos Int. 2001; 12:936–41. [PubMed: 11804020]
44. Westerlind KC, Wronski TJ, Ritman EL, Luo ZP, An KN, Bell NH, Turner RT. Estrogen regulates the rate of bone turnover but bone balance in ovariectomized rats is modulated by prevailing mechanical strain. Proc Natl Acad Sci U S A. 1997; 94:4199–204. [PubMed: 9108129]
45. Ding WG, Wei ZX, Liu JB. Reduced local blood supply to the tibial metaphysis is associated with ovariectomy-induced osteoporosis in mice. Connect Tissue Res. 2011; 52:25–9. [PubMed: 20497029]
46. Teti A, Zallone A. Do osteocytes contribute to bone mineral homeostasis? Osteocytic osteolysis revisited Bone. 2009; 44:11–6.
47. Qing H, Ardeshirpour L, Pajevic PD, Dusevich V, Jähn K, Kato S, Wysolmerski J, Bonewald LF. Demonstration of osteocytic perilacunar/canalicular remodeling in mice during lactation. J Bone Miner Res. 2012; 27:1018–29. [PubMed: 22308018]
48. Tazawa K, Hoshi K, Kawamoto S, Tanaka M, Ejiri S, Ozawa H. Osteocytic osteolysis observed in rats to which parathyroid hormone was continuously administered. J Bone Miner Metab. 2004; 22:524–9. [PubMed: 15490261]
49. Lane NE, Yao W, Balooch M, Nalla RK, Balooch G, Habelitz S, Kinney JH, Bonewald LF. Glucocorticoid treated mice have localized changes in trabecular bone material properties and osteocyte lacunar size that are not observed in placebo-treated or estrogen-deficient mice. J Bone Miner Res. 2006; 21:466–76. [PubMed: 16491295]
50. Tang SY, Herber RP, Ho SP, Alliston T. Matrix metalloproteinase-13 is required for osteocytic perilacunar remodeling and maintains bone fracture resistance. J Bone Miner Res. 2012; 27:1936–50. [PubMed: 22549931]
51. Plotkin LI, Mathov I, Aguirre JI, Parfitt AM, Manolagas SC, Bellido T. Mechanical stimulation prevents osteocyte apoptosis: requirement of integrins, Src kinases, and ERKs. Am J Physiol Cell Physiol. 2005; 289:C633–43. [PubMed: 15872009]
52. Zaman G, Saxon LK, Sunters A, Hilton H, Underhill P, Williams D, Price JS, Lanyon LE. Loading-related regulation of gene expression in bone in the contexts of estrogen deficiency, lack of estrogen receptor alpha and disuse. Bone. 2010; 46:628–42. [PubMed: 19857613]
53. Kennedy OD, Herman BC, Laudier DM, Majeska RJ, Sun HB, Schaffler MB. Activation of resorption in fatigue-loaded bone involves both apoptosis and active pro-osteoclastogenic signaling by distinct osteocyte populations. Bone. 2012; 50:1115–22. [PubMed: 22342796]
54. Lanyon L, Skerry T. Postmenopausal osteoporosis as a failure of bone's adaptation to functional loading: a hypothesis. J Bone Miner Res. 2001; 16:1937–47. [PubMed: 11697789]

Highlights

- This study examined the combined effect of estrogen deficiency and external loading on interstitial fluid flow around osteocytes.
- Mechanical loading enhanced labeling of osteocyte lacunae with injected tracer; ovariectomy further enhanced tracer movement in cancellous bone.
- The altered interstitial fluid flow around osteocytes is likely related to nanostructural matrix-mineral changes recently demonstrated in estrogen-deficient rats.
- Findings demonstrate a functional difference in interstitial fluid flow that could affect transmission of mechanical loads to the osteocyte.

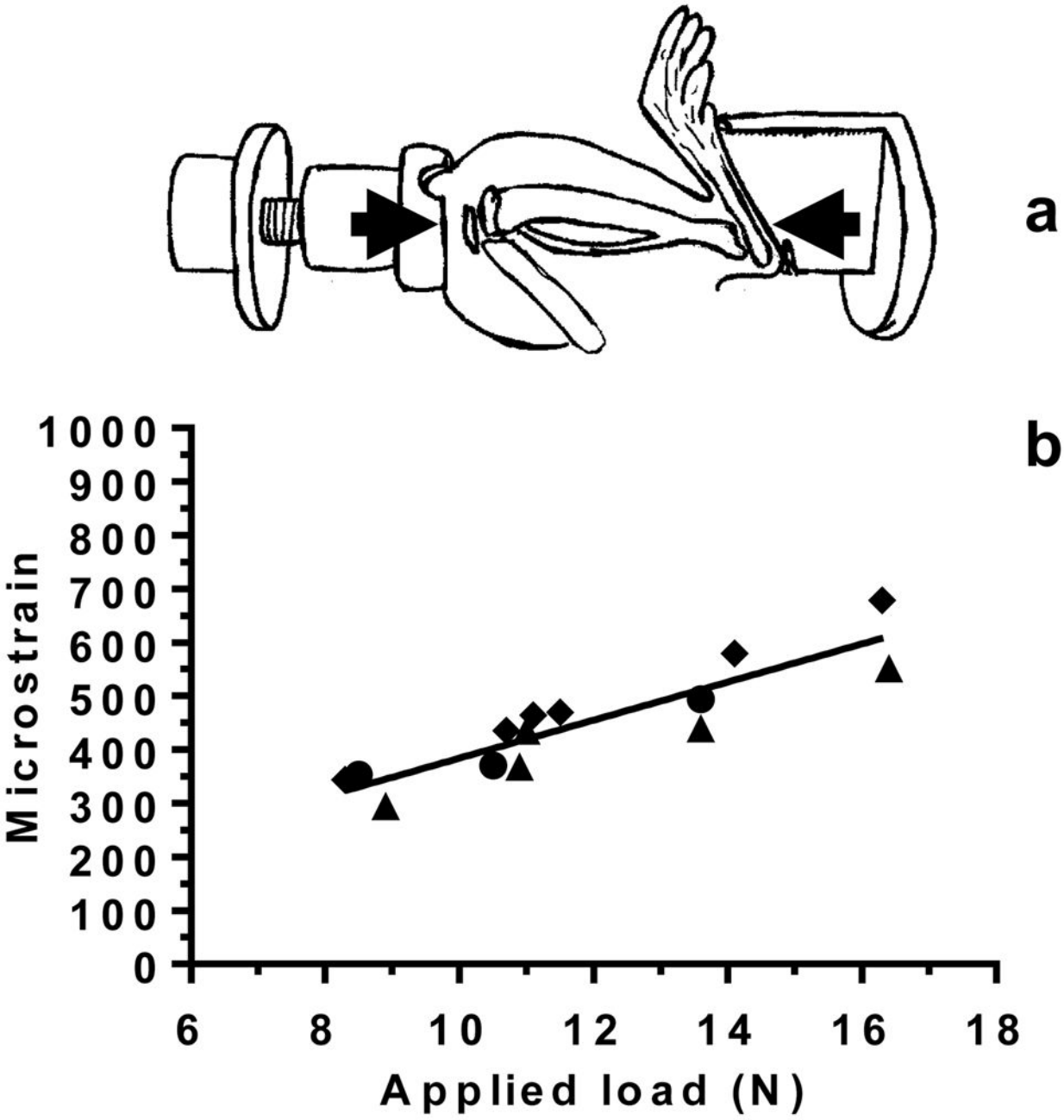

Figure 1.

(a) Sinusoidal loading was applied non-invasively to the rat lower hindlimb, which was constrained between a custom-made knee cup and foot holder. The lower limb was compressed in the direction indicated by the arrows. (b) Strain-gage calibration of the loading device using control rats (n=3; each rat represented by a symbol, ● ▲ ◆) illustrates the relationship between applied load (N) and measured deformation (microstrain) of the proximal tibia. After tracer injection, an applied load of 14 N, which engenders ~500 microstrain at the medial proximal diaphysis, was applied at 1 Hz to mimic slow walking.

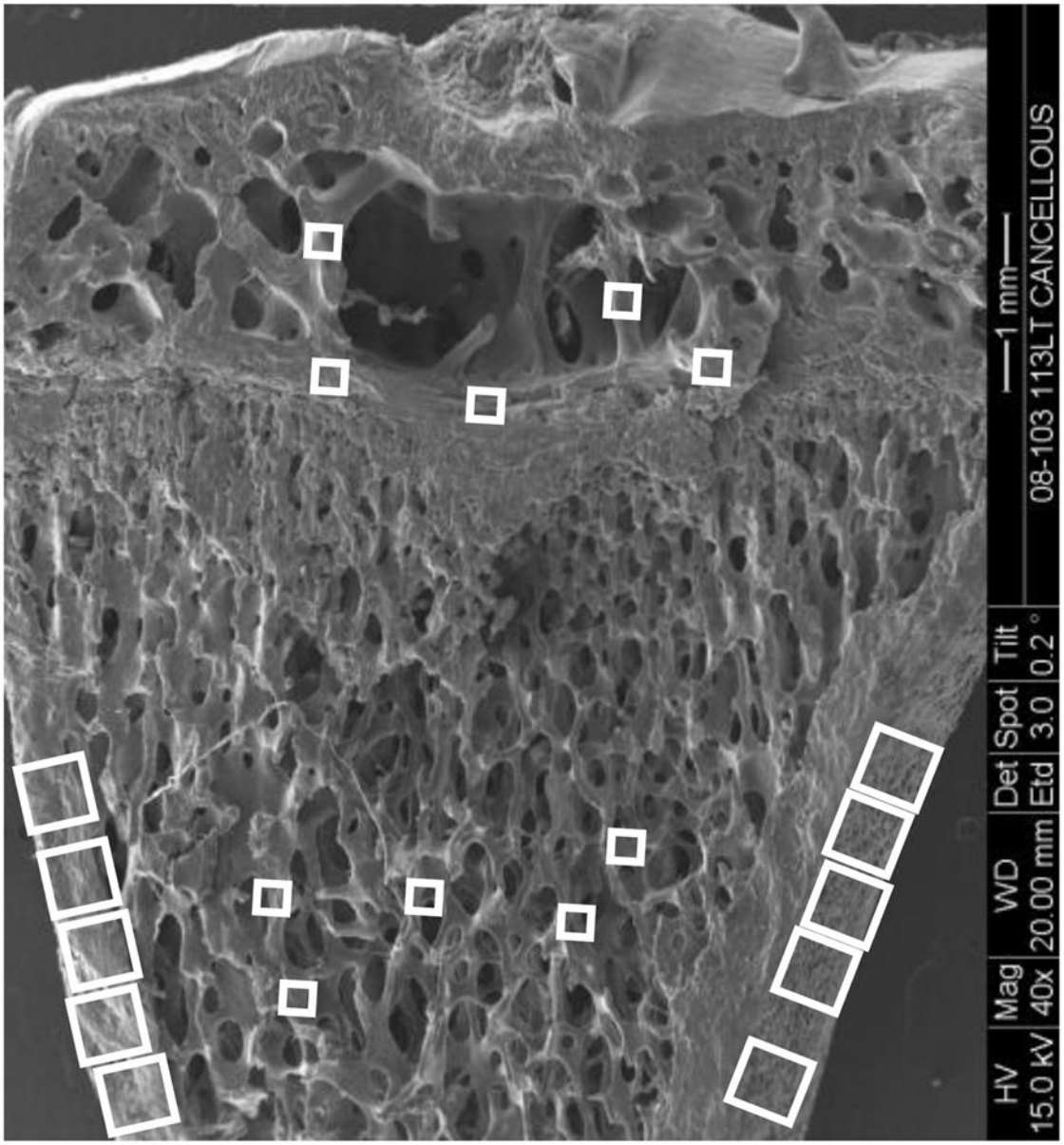

Figure 2.

Scanning electron microscopy image of a rat proximal tibia frontal section illustrating where the cortical and cancellous bone confocal images were taken to assess osteocyte lacunae labeled with injected tracer. For the metaphyseal region, five cancellous bone image samples (187.5 μm × 187.5 μm images, smaller boxes) were taken in the region spanning 1 to 3 mm distal to the growth plate; primary spongiosa were not included. Ten cortical metaphyseal image samples (375 μm × 375 μm images, larger boxes) were taken from the cortex region. For the epiphyseal region, three image samples were taken right above the growth plate, without including any region of the growth plate, to ensure consistency in sampling, and two additional regions of interest were sampled more proximally (187.5 μm × 187.5 μm images, smaller boxes).

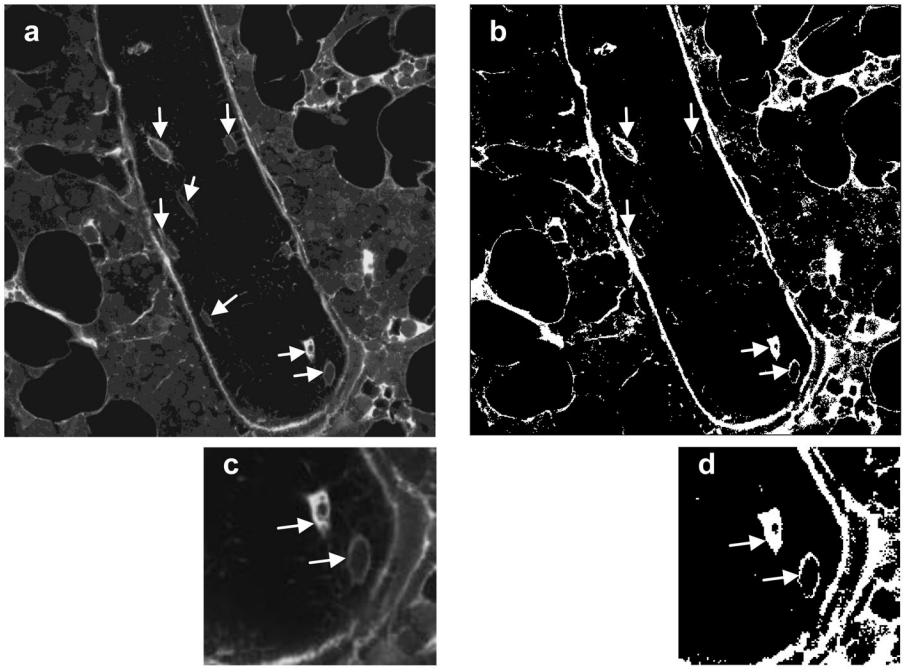

Figure 3.

Tracer transport through the lacunar-canalicular system was assessed using confocal microscopy to identify osteocyte lacunae considered labeled in both loaded and unloaded tibiae. (a) A typical grayscale image of cancellous bone of the metaphysis. The trabecula shown is surrounded by bone marrow, and the fully visible osteocytes are indicated with arrows. (b) The same image after thresholding; labeled osteocyte lacunae are marked with arrows. (c) Higher magnification of the image in (a) showing two osteocytes, and (d) the same image after thresholding. The arrows in (d) indicate that both osteocytes satisfied the criteria to be counted as labeled (osteocyte lacunae presenting at least 80% of the lacunar space stained or 80% of the periphery of the lacuna stained).

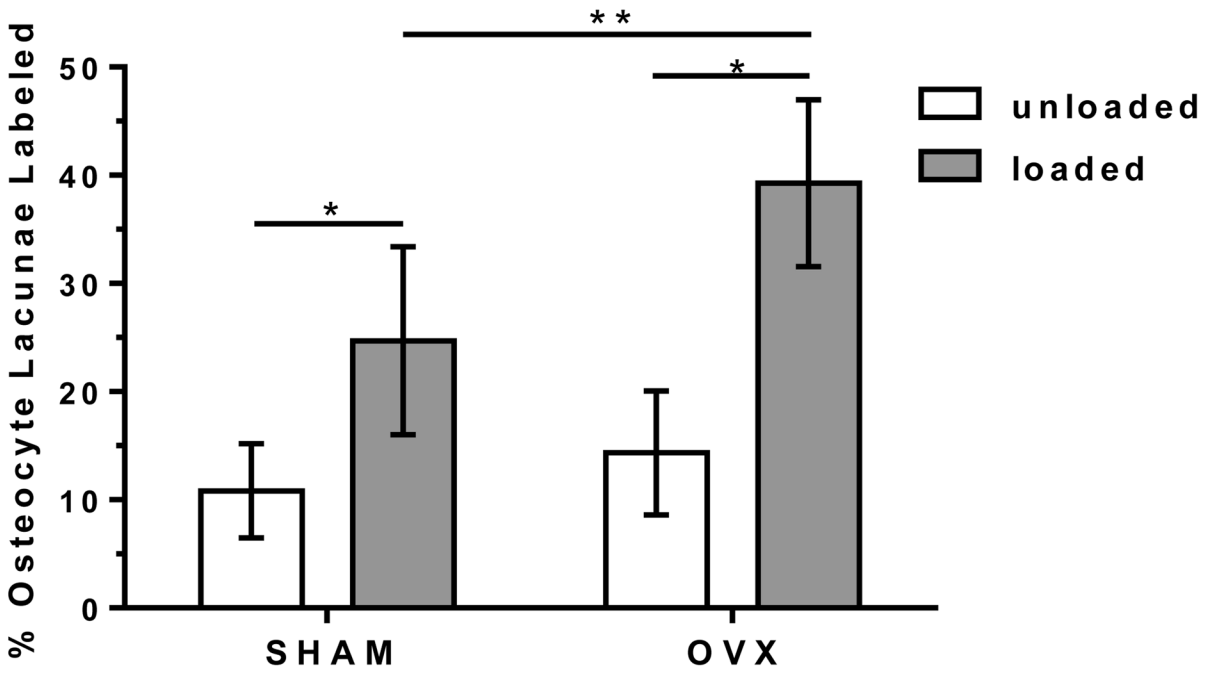

Figure 4.

The percentage of osteocyte lacunae labeled with injected tracer (mean ± SD) for the SHAM and OVX groups with the measurements at three anatomical locations (cortical metaphysis, cancellous metaphysis, and cancellous epiphysis) pooled for each animal for the loaded and contralateral, unloaded tibiae.

* significant difference compared to unloaded in same group ($p < 0.05$);

** significant difference compared to loaded SHAM ($p < 0.05$).

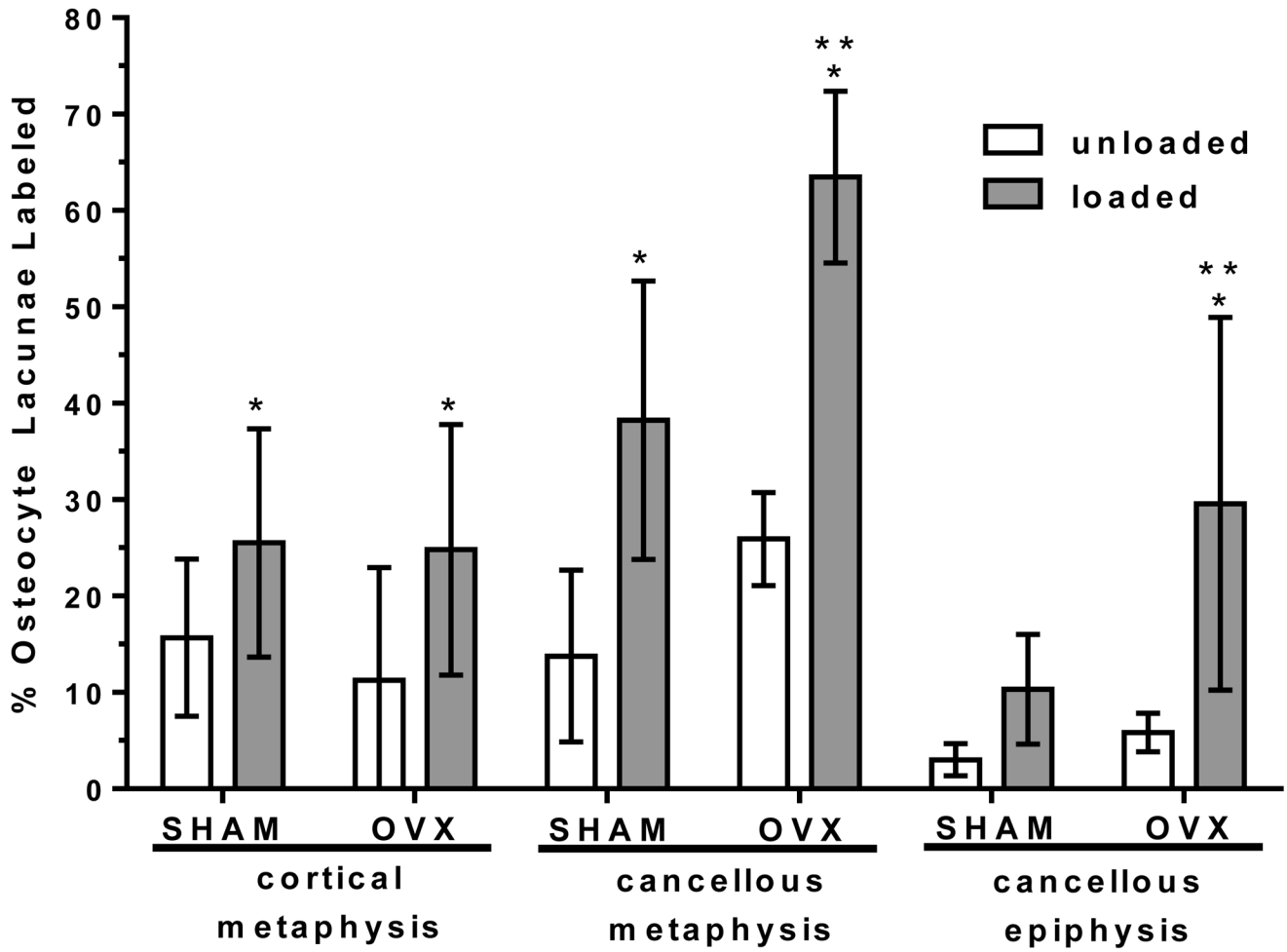

Figure 5.

The percentage of osteocyte lacunae labeled with injected tracer (mean ± SD) for the SHAM and OVX groups for the three anatomical locations analyzed: cortical metaphysis, cancellous metaphysis, and cancellous epiphysis in the loaded and contralateral, unloaded tibiae.

* significant difference compared to unloaded in same group ($p < 0.05$);

** significant difference compared to loaded SHAM at same location ($p < 0.05$).